INTERNATIONAL JOURNAL FOR NUMERICAL METHODS IN FLUIDS, VOL. 5, 169–189 (1985)

ON THE SOLUTION FOR STEADY STATE AND TIME DEPENDENT FLOWS IN CERTAIN CHANNELS WITH SMALL WALL CURVATURE

G. A. GEORGIOU

Department of Mechanical Engineering, University College, London WC1E 7JE, U.K.

AND

C. P. ELLINAS

J. P. Kenny & Partners, Burne House, 88–89 High Holborn, London WC1V 6LS, U.K.

SUMMARY

An asymptotic scheme is presented for the solution of the steady state and time dependent stream functions for flows in symmetric curved walled channels. In this scheme a class of non-linear Jeffery–Hamel solutions appear at $O(1)$, and thus provide the first approximation to the steady state stream function. This class of Jeffery–Hamel solutions are evaluated by using a simple perturbation about Poiseuille flow.

The classic Orr–Sommerfeld eigenproblem appears at $O(1)$ in the asymptotic development of the time dependent stream function, but here there is a slow streamwise dependence. This eigenvalue problem, for a complex wave number, is solved using an algorithm which automatically provides an initial guess which is then used to iterate to the correct eigenvalue.

Higher order terms in the asymptotic development, for both the steady state and time dependent stream functions, are evaluated to provide a solution for the total stream function.

KEY WORDS Jeffery–Hamel Orr–Sommerfeld

1. INTRODUCTION

In this investigation we consider flows in curved walled channels, and express the Navier–Stokes equations for a viscous incompressible fluid in terms of Fraenkel's[1,2] general orthogonal co-ordinates. In the results presented here, the curvatures of the channel walls are constant in sign.

We consider first a steady state spatially dependent stream function $\Omega(\xi, \eta)$ (where ξ and η represent the downstream and transverse co-ordinates respectively), and present the analysis in Section 3. Using Fraenkel's[1,2] small wall curvature theory, a class of Jeffery–Hamel solutions,[3,4] which are exact for channels with plane walls[5] (henceforth straight walls), are used as a first approximation for channels with slowly varying walls. Hence, the asymptotic development for $\Omega(\xi, \eta)$ is expressed in ascending powers of a small parameter, where these non-linear Jeffery–Hamel solutions appear at first order. The slow variation of $\Omega(\xi, \eta)$ in the streamwise direction is expressed in terms of a slow variable $\sigma_1 = \varepsilon^{1/2}\xi$,[6] and these non-parallel slow variations along with curvature are accounted for by higher order terms.

The class of Jeffery–Hamel solutions are perturbed about linear functions, the first of which represents plane Poiseuille flow.[7] These perturbation functions are unique for every Jeffery–Hamel solution here, and need only be computed once. The linear differential equations satisfied by the

0271–2091/85/02 0169–21$02.10

Received 25 November 1983
Revised 16 April 1984

perturbation functions are discretized using central difference formulae of $O(h^4)$. However, in order to define these functions throughout the whole problem domain it is necessary to use mixed order difference formulae in the boundary conditions. The numerical scheme to evaluate a class of Jeffery–Hamel solutions is found to be economic even for a large number of perturbation functions. The final results agree very well with other numerical results[8,9] and with results computed from analytic expressions.[1,2]

The linear differential equations for the higher order functions in the asymptotic development for $\Omega(\xi, \eta)$, are discretized using a similar finite difference scheme to that used for the perturbation functions. The set of matrix equations obtained have a common L.H.S. with a different R.H.S. vector for each of these higher order functions.

A small disturbance $\Phi(\xi, \eta, t)$ to the steady state $\Omega(\xi, \eta)$ is considered in Section 4. The resulting linear differential equations, with slowly varying coefficients, independent of time, suggest that fixed frequency disturbances of form $\phi(\sigma_1, \eta)\exp(\mathrm{i}(\theta(\xi) - \beta t))$ are appropriate solutions for $\Phi(\xi, \eta, t)$. The slow variation in the ξ-direction is allowed for through the complex wave number $k(\sigma_1)$ where $\mathrm{d}\theta/\mathrm{d}\xi = k(\sigma_1)$. This form to $\Phi(\xi, \eta, t)$, with spatially varying amplitude,[10] is a modification to the quasi-parallel approach which would ignore the slow variation in the ξ-direction.[8,11]

The asymptotic development for $\Phi(\xi, \eta, t)$ yields the classic Orr–Sommerfeld eigenproblem at lowest order, where here the coefficients exhibit the slow variation with ξ.[8] In fact this problem has formed the basis for linearized stability theory for over half a century.[12–15] Earlier analytical methods for its solution have been superseded by numerical ones, and an important investigation is referenced in Reference 16. In the present investigation, the necessary characteristic equation defining the eigenrelation is approximated by a quartic equation with complex coefficients. This quartic yields a consistent and good initial guess which is used in a modified quadratic Newton–Raphson scheme to iterate to the correct eigenvalue.

The solution of the higher order disturbance equations implied by the asymptotic development for $\Phi(\xi, \eta, t)$ is described in general form, and Runge–Kutta schemes of order four are used to find particular solutions to these equations.

The potential to carry out a full stability analysis is discussed in Section 5, and the application of the theory to channels with more general curvature is exemplified in Figures 7 and 8.

2. THE PROBLEM

Consider the Navier–Stokes equations in two dimensions for an incompressible viscous fluid. We can express these equations using general orthogonal co-ordinates (a_1, a_2) in terms of the dimensional stream function $\hat{\Psi}$,[17] which is given by

$$\frac{\partial}{\partial T}(\nabla^2\hat{\Psi}) + \frac{1}{h_1 h_2}\left[\frac{\partial\hat{\Psi}}{\partial a_2}\frac{\partial}{\partial a_1}(\nabla^2\hat{\Psi}) - \frac{\partial\hat{\Psi}}{\partial a_1}\frac{\partial}{\partial a_2}(\nabla^2\hat{\Psi})\right] = \nu\nabla^4\hat{\Psi} \tag{1}$$

where T is time, h_1 and h_2 are the scalar factors and

$$\nabla^2 = \frac{1}{h_1 h_2}\left[\frac{\partial}{\partial a_1}\left(\frac{h_2}{h_1}\frac{\partial}{\partial a_1}\right) + \frac{\partial}{\partial a_2}\left(\frac{h_1}{h_2}\frac{\partial}{\partial a_2}\right)\right]$$

The co-ordinate system to be used here is in Fraenkel's[1,2] notation, and this is recalled and summarized.

Let (X, Y) denote the dimensional system of Cartesian co-ordinates where the following transformation is used:

$$Z = Z(\zeta) \text{ where } Z = X + \mathrm{i}Y \text{ and } \zeta = \xi + \mathrm{i}\eta$$

We also define H and ϑ by

$$\frac{dZ}{d\zeta} = H(\xi,\eta)\exp(i\vartheta(\xi,\eta)) \tag{2}$$

Here, H is a dimensional scaling factor, that is an arc length dS in the Z plane is H times the corresponding arc length in the ζ plane, $|dZ| = H|d\zeta|$. The parameter ϑ is the angle between corresponding line elements, so that $\arg(dZ) - \arg(d\zeta) = \vartheta$. Let

$$\frac{d}{d\zeta}\left(\ln\left(\frac{dZ}{d\zeta}\right)\right) = \kappa(\xi,\eta) - i\lambda(\xi,\eta) = \mu(\zeta) \tag{3}$$

Using (2) and (3), the Cauchy–Riemann equations yield

$$\kappa = \frac{1}{H}\frac{\partial H}{\partial \xi} = \frac{\partial \vartheta}{\partial \eta} \tag{4a}$$

$$\lambda = \frac{1}{H}\frac{\partial H}{\partial \eta} = -\frac{\partial \vartheta}{\partial \xi} \tag{4b}$$

where κ/H and λ/H are the curvatures in the Z-plane of the co-ordinate lines corresponding to $\xi =$ constant, and $\eta =$ constant, respectively. The form of (1) can now be transformed in terms of Fraenkel's general orthogonal co-ordinates (ξ,η) where $h_1 = h_2 = H$, $a_1 = \xi$ and $a_2 = \eta$. The non-dimensional equation is found by setting

$$\hat{\Psi} = M\Psi; \quad H = bh; \quad T = \frac{b^2 t}{M}; \quad Z = bz \tag{5}$$

where M is defined to be half the volumetric flow rate per unit depth normal to the (ξ,η) plane, $2b$ is approximately the throat width of the channel at $\xi = 0$, and it can be shown that $2H$ is

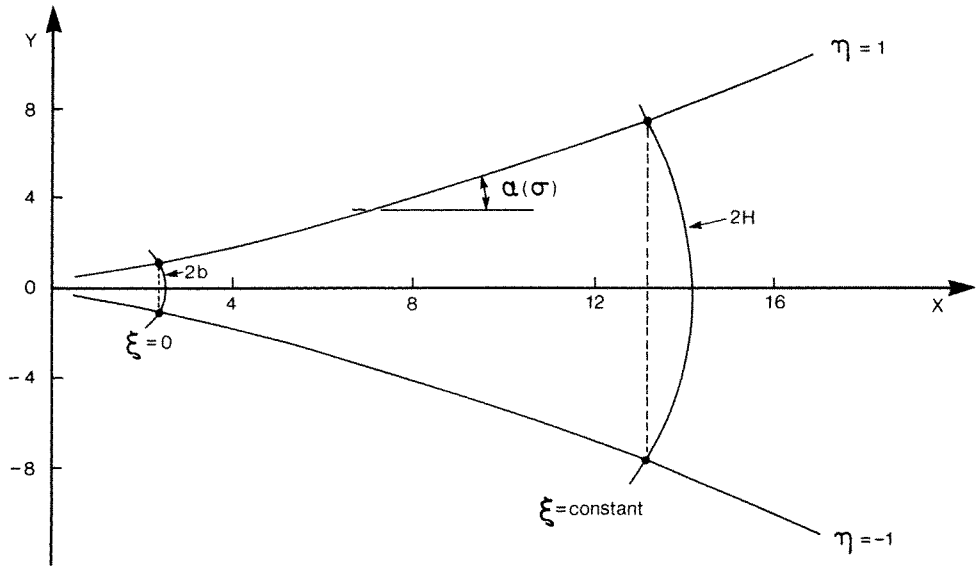

Figure 1. A curved walled channel given by $\alpha(\tau) = \varepsilon^{1/2} + \varepsilon^{1/2} m\tau$ for $m = 1$ and $\varepsilon^{1/2} = 0{\cdot}4$

approximately the width of the channel corresponding to $\xi = \text{constant}$.[1,2] The channel shape and notation are shown in Figure 1. Thus (1) can be shown to take the form

$$\left\{\frac{1}{R}\left(D^2 - 4\left(\kappa\frac{\partial}{\partial\xi} + \lambda\frac{\partial}{\partial\eta}\right) + 4(\kappa^2+\lambda^2)\right) - h^2\frac{\partial}{\partial t} - \left(\frac{\partial\Psi}{\partial\eta}\frac{\partial}{\partial\xi} - \frac{\partial\Psi}{\partial\xi}\frac{\partial}{\partial\eta} - 2\kappa\frac{\partial\Psi}{\partial\eta} + 2\lambda\frac{\partial\Psi}{\partial\xi}\right)\right\} D^2\Psi = 0 \tag{6}$$

where $D^2 = \partial^2/\partial\eta^2 + \partial^2/\partial\xi^2$ and the boundary conditions are given by

$$\Psi = \pm 1, \quad \text{at} \quad \eta = \pm 1 \tag{7}$$

and

$$\frac{\partial\Psi}{\partial\eta} = 0, \quad \text{at} \quad \eta = \pm 1 \tag{8}$$

The Reynolds number R has been defined by M/v. It is necessary to define R in this way so that it will not vary from station to station in the channel.[5]

The condition (7) follows from the definitions of Ψ and M earlier, and (8) is the no slip condition at the walls of the channel. It should be emphasized that (7) and (8) do not necessarily imply that Ψ is an odd (antisymmetric) function, but are consistent with such an assumption.

It is assumed that Ψ, the total stream function, is given by

$$\Psi(\xi,\eta,t) = \Omega(\xi,\eta) + \Phi(\xi,\eta,t) \tag{9}$$

where $\Omega(\xi,\eta)$ is called the steady state stream function and $\Phi(\xi,\eta,t)$ is called the time dependent stream function. In addition, the functions Ω and Φ are chosen to be the odd and even parts of Ψ, respectively, with respect to η.

3. THE STEADY STATE EQUATIONS

3.1. Theory

The steady state equation for $\Omega(\xi,\eta)$ may be deduced from (6), it is given by

$$\left\{\frac{1}{R}\left(D^2 - 4\left(\kappa\frac{\partial}{\partial\xi} + \lambda\frac{\partial}{\partial\eta}\right) + 4(\kappa^2+\lambda^2)\right) - \left(\frac{\partial\Omega}{\partial\eta}\frac{\partial}{\partial\xi} - \frac{\partial\Omega}{\partial\xi}\frac{\partial}{\partial\eta} - 2\kappa\frac{\partial\Omega}{\partial\eta} + 2\lambda\frac{\partial\Omega}{\partial\xi}\right)\right\} D^2\Omega = 0 \tag{10a}$$

and

$$\Omega = \pm 1, \quad \text{at} \quad \eta = \pm 1; \quad \frac{\partial\Omega}{\partial\eta} = 0, \quad \text{at} \quad \eta = \pm 1 \tag{10b}$$

It can be seen that (10a) is non-linear.

Fraenkel's[1,2] asymptotic development of the solution to (10a) depends on a parameter ε, assumed to be small, such that

$$\varepsilon\zeta = \tau; \quad \varepsilon\xi = \sigma; \quad \tau = \sigma + i\varepsilon\eta \tag{11}$$

In addition he proposes

$$\mu(\zeta) = \alpha(\tau) \tag{12}$$

These relations ensure that μ varies slowly with ζ and is nearly real. The geometric significance of function $\alpha(\tau)$ is that it may be shown to be approximately equal to the real semi-divergence angle of

the channel wall (see Figure 1). Fraenkel[1,2] showed that the choice of $\alpha(\tau)$ depends crucially on two necessary conditions to be satisfied by R and ε, these are

$$R\alpha = O(1) \tag{13}$$

and

$$R\varepsilon < O(1) \tag{14}$$

With these conditions Fraenkel ensured that a class of Jeffery–Hamel solutions for a straight walled channel appear as the first order terms in the solution for the curved walled channel. Fraenkel's asymptotic solution of (10a) is based on $\varepsilon \to 0$ with σ, η fixed.

In the present case the channel chosen is characterized by

$$\alpha(\tau) = \varepsilon^{1/2} + \varepsilon^{1/2} m\tau \tag{15}$$

The choice of the parameters σ and ε, although justified for the steady state case, leads to problems of unboundedness in the time dependent analysis. For this reason the introduction of a new slow variable, σ_1, becomes necessary. This is given by

$$\sigma_1 = \varepsilon^{1/2}\xi \tag{16a}$$

which implies

$$\sigma = \varepsilon^{1/2}\sigma_1 \tag{16b}$$

The asymptotic analysis will now be based on $\varepsilon^{1/2} \to 0$ with σ_1 and η fixed. Exact expressions for κ and λ in terms of $\varepsilon^{1/2}$ can be obtained from (3) and (15). The choice of $\alpha(\tau)$ and a parameter v such that

$$R = \frac{v}{\varepsilon^{1/2}} \tag{17}$$

ensures that (13) and (14) are satisfied.

It is shown in Appendix I that the asymptotic expansion for $\Omega(\xi, \eta)$ takes the form

$$\Omega(\xi, \eta; v, m) = G_0 + \varepsilon^{1/2}(G_3 + \sigma_1 G_1) + \varepsilon(G_5 + \sigma_1 G_4 + \sigma_1^2 G_1) + \cdots \tag{18}$$

The equation for G_0 is given by

$$\frac{\mathrm{d}^4 G_0}{\mathrm{d}\eta^4} + 2v\frac{\mathrm{d}G_0}{\mathrm{d}\eta}\frac{\mathrm{d}^2 G_0}{\mathrm{d}\eta^2} = 0 \tag{19a}$$

where

$$G_0 = \pm 1; \quad \frac{\mathrm{d}G_0}{\mathrm{d}\eta} = 0, \quad \text{at} \quad \eta = \pm 1 \tag{19b}$$

The first order term, G_0, represents a class of Jeffery–Hamel solutions for the straight walled channel. The equations for the remaining functions may be expressed in the general form

$$\frac{\mathrm{d}^4 G_i}{\mathrm{d}\eta^4} + 2v\frac{\mathrm{d}}{\mathrm{d}\eta}\left(\frac{\mathrm{d}G_0}{\mathrm{d}\eta}\frac{\mathrm{d}G_i}{\mathrm{d}\eta}\right) = F(G_j), \quad (j = i-1, i-2, \ldots, 0) \tag{20a}$$

where

$$G_i = \frac{\mathrm{d}G_i}{\mathrm{d}\eta} = 0, \quad \text{at} \quad \eta = \pm 1 \quad (i \geqslant 1) \tag{20b}$$

Explicit expressions for $F(G_j)$ may be found in References 18 and 19.

One result from the assumption that $\Omega(\xi, \eta)$ is odd is that the functions $G_i (i \geqslant 0)$ are also odd.

The scheme used to determine G_0 is essentially a perturbation about Poiseuille flow, where G_0 is

expanded as a Taylor series in power of v.

$$G_0(\eta) = w_0(\eta) + w_1(\eta)v + w_2(\eta)\frac{v^2}{2!} + \cdots + \frac{w_r(\eta)v^r}{r!} + \cdots \tag{21}$$

where the w_r's are called perturbation functions. The function w_0 represents Poiseuille flow.

It is interesting to note here that the solution to the problem follows a natural physically based sequence. The solution of the curved walled channel is obtained by perturbing about the straight walled channel, the solution of which in turn is based on perturbing about Poiseuille flow. Thus the three stages, from parallel to straight to curved walled channels are naturally introduced as steps in obtaining the final solutions.

Since G_0 is an odd function, the boundary conditions in (19b) may be rewritten as

$$G_0(0) = 0, \quad \frac{dG_0}{d\eta}(0) = 0; \quad G_0(1) = 1, \quad \frac{dG_0}{d\eta}(1) = 0 \tag{22}$$

On substituting (21) into (19a) and comparing powers of v, the following expressions are obtained for the perturbation functions w_r.

$$\frac{d^4 w_r}{d\eta^4} = 0 \tag{23a}$$

where

$$w_0(0) = \frac{d^2 w_0}{d\eta^2}(0) = 0; \quad w_0(1) = 1, \quad \frac{dw_0}{d\eta}(1) = 0 \tag{23b}$$

and

$$\frac{d^4 w_r}{d\eta^4} = -2\sum_{s=1}^{r}\left[\frac{r!}{(r-s)!(s-1)!}\frac{dw_{s-1}}{d\eta}\frac{d^2 w_{r-s}}{d\eta^2}\right]; \quad r \geqslant 1 \tag{24a}$$

where

$$w_r(0) = \frac{d^2 w_r}{d\eta^2}(0) = 0; \quad w_r(1) = \frac{dw_r}{d\eta}(1) = 0 \tag{24b}$$

3.2. *The numerical solution*

These linear differential equations may be discretized using central difference expressions of $O(h^4)$, given in Appendix II. In matrix form they become

$$[A]\{w_r\} = \{B_r\}; \quad r \geqslant 0 \tag{25}$$

The banded matrix $[A]$ containing the finite difference coefficients is common to all the w_r's, and hence needs to be generated only once. The functions are defined at the grid points 1 to N inside the problem domain, that is $\eta = 0$ to $\eta = 1$, by the application of the discretized forms of either equations (23a) or (24a) at these points (see Figure 2).

When using central difference expressions of $O(h^4)$ problems may be encountered near to or on the boundaries. To illustrate these problems we refer to Figure 2. The application of the discretized

Figure 2. A finite difference grid for half the channel

forms of either equations (23a) or (24a) (see Appendix II) at $\eta = 0$ and $\eta = 1$, requires the definition of the functions at auxiliary points outside the problem domain, as shown in Figure 2. The antisymmetric conditions at $\eta = 0$ are sufficient to define these auxiliary points. However, at $\eta = 1$ only two boundary conditions are available, as shown by equations (23b) or (24b). This difficulty can be overcome by eliminating the grid point $(N + 3)$ from the finite difference solution. This can be achieved by using mixed central-backward difference expressions for the fourth derivative on the boundary, so that the point $(N + 3)$ does not appear in the solution. However, numerical instabilities and associated convergence problems were introduced with this approach.[18]

An alternative method, discussed in more detail in Reference 18, involves the derivation of an additional boundary condition that can be used to define point $(N + 3)$. This can be obtained by differentiating equations (23a) and (24a) once with respect to η, so that

$$\frac{d^5 w_0}{d\eta^5} = 0, \quad \text{at} \quad \eta = 1 \tag{26a}$$

and

$$\frac{d^5 w_r}{d\eta^5} = -2 \sum_{s=1}^{r} \left[\frac{r!}{(r-s)!(s-1)!} \frac{d^2 w_{s-1}}{d\eta^2} \frac{d^2 w_{r-s}}{d\eta^2} \right], \quad \text{at} \quad \eta = 1; \quad r \geqslant 1 \tag{26b}$$

The dilemma of using the discretized form of equations (26), using finite differences of $O(h^4)$, is that they involve an additional point $(N + 4)$, which again is undefined. To overcome this problem, finite difference expressions were derived for the relevant derivatives of w_r from the same polynomial, as shown in Appendix III. The consistency of this method lies in the fact that all derivatives have been derived from a polynomial of $O(8)$. The derived finite difference expressions in Appendix III involve only three auxiliary points at $(N + 1)$, $(N + 2)$ and $(N + 3)$, which are now completely defined by the use of the discretized forms of equations (23b) and (26a) or (24b) and (26b). This scheme was found to produce results for G_0 which agreed to four significant figures with exact analytic based on elliptic functions. [1,2] Such results are shown in Table I.

The advantage of the present method in comparison to the other available methods of solution, such as Runge–Kutta schemes, is that the perturbation functions $w_r(\eta)$ need be obtained only once, and G_0 can then be simply computed using equation (21) for any value of v.

Once G_0 has been computed, solutions for $G_j (j = 1, \ldots, 5)$ may be obtained by discretizing equation (20) using a scheme similar to that discussed for G_0. The resulting discretized linear algebraic equations take a form similar to equation (25). In this, the left hand side matrix need be constructed only once. Solutions for different G_j may be obtained after computing the relevant right hand side vector, using equation (20).

Table I. A class of Jeffery–Hamel profiles at $\eta = 0$, by elliptic functions, and the present perturbation scheme, for a range of v

v	Elliptic (Fraenkel)	Perturbation (present)
3·13	1·781	1·781
3·572	1·856	1·856
3·904	1·926	1·926
4·093	1·973	1·973
4·295	2·031	2·031
4·712	2·188	2·188
5·102	2·429	2·429

Table II. Results of G_0 and some derivatives at $\eta = 0{\cdot}5$, using 80 η steps with $v = 5$, for a different number of perturbation terms in the straight walled channel

Perturbation terms	$G_0(0{\cdot}5)$	$G_0'(0{\cdot}5)$	$G_0''(0{\cdot}5)$	$G_0'''(0{\cdot}5)$
8	0·856785	0·892198	− 3·505546	4·112094
16	0·873550	0·859079	− 3·664425	5·208263
32	0·878250	0·849729	− 3·707526	5·510530
40	0·876610	0·849011	− 3·710787	5·533522
48	0·878742	0·848749	− 3·711974	5·541906
56	0·878792	0·848648	− 3·712430	5·545129
64	0·878813	0·848607	− 3·712612	5·546515

Table III. Results of G_0 and some derivatives at $\eta = 0{\cdot}6$, using 64 perturbation terms with $v = 5$, for a different number of η steps in the straight walled channel

Number of η steps	$G_0(0{\cdot}6)$	$G_0'(0{\cdot}6)$	$G_0''(0{\cdot}6)$	$G_0'''(0{\cdot}6)$
20	0·946175	0·509933	− 3·030069	7·844196
30	0·946156	0·509661	− 3·029546	7·848162
40	0·946152	0·509614	− 3·029455	7·848649
50	0·946151	0·509602	− 3·029430	7·848763
60	0·946151	0·509597	− 3·029421	7·848800
70	0·946151	0·509595	− 3·029417	7·848815
80	0·946151	0·509594	− 3·029415	7·848822

Table IV. Results of G_5 and some derivatives at $\eta = 0{\cdot}6$, using 64 perturbation terms with $v = 5$, for a different number of η steps in the curved walled channel

Number of η steps	$G_5(0{\cdot}6)$	$G_5'(0{\cdot}6)$	$G_5''(0{\cdot}6)$	$G_5'''(0{\cdot}6)$
20	3·041040	− 9·745376	− 16·160815	212·483875
30	3·011692	− 9·642115	− 16·079510	209·804742
40	3·006590	− 9·624146	− 16·065167	209·333534
50	3·005175	− 9·619519	− 16·061159	209·202239
60	3·004662	− 9·617354	− 16·059703	209·154608
70	3·004442	− 9·616576	− 16·059074	209·134069
80	3·004334	− 9·616197	− 16·058766	209·124049

A parametric study was carried out and the results, which are summarized in Tables II–IV, showed that for an extreme value of v, 64 perturbation in equation (21) and 80 η steps were necessary for convergence to at least four significant figures for $G_i (i = 0, \ldots, 5)$, and their first three derivatives, where G_0' denotes the first derivative w.r.t. η. Computationally the scheme was found to be both economic and efficient.

The steady state stream function Ω may now be computed using equation (18) for the complete η range and the required values of the downstream variable σ_1.

The convergence of the truncated expansion for Ω, given by equation (18), up to the $O(\varepsilon)$ term, is examined in Figures 3 and 4. This is achieved by comparing the present solution with that obtained

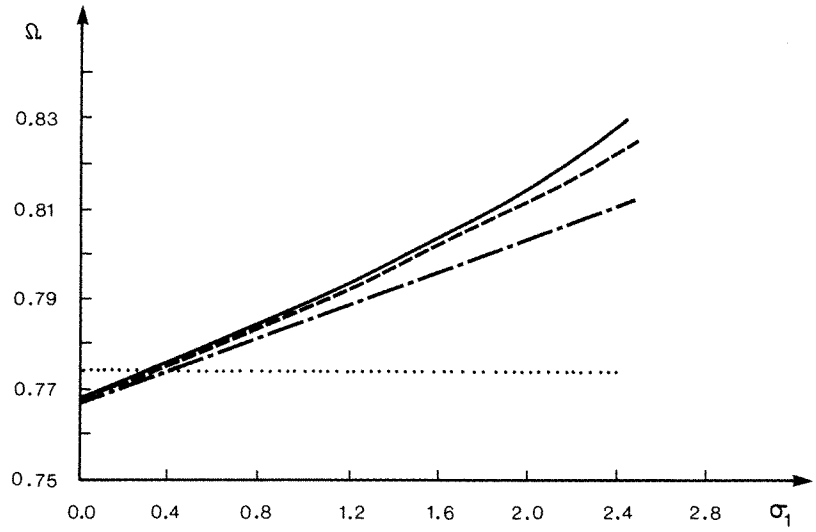

Figure 3. The steady state stream function in the downstream direction at different orders for $v = 3{\cdot}572$; $R = 30$, $m = 1$.....$O(1)$, —·—$O(\varepsilon^{1/2})$, ------$O(\varepsilon)$, ——$O(\varepsilon^{3/2})$

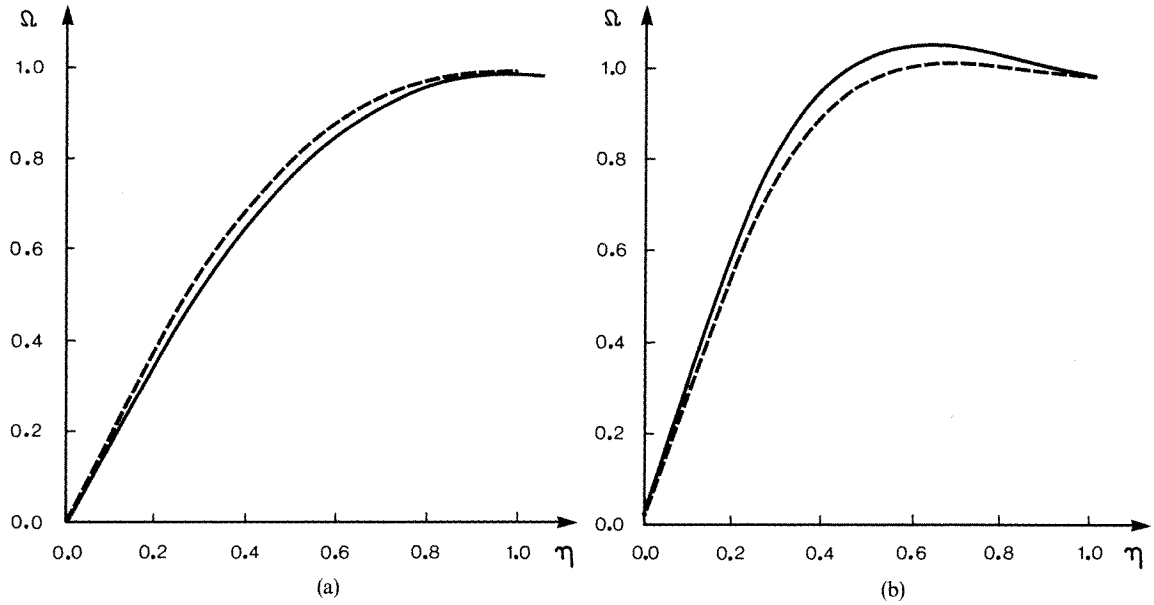

Figure 4. The steady state stream function in the transverse direction at different orders for $v = 4{\cdot}71$; $R = 30$, $m = 1$, at $\sigma_1 = 0{\cdot}0$ and $\sigma_1 = 1{\cdot}6$. -----$O(\varepsilon)$, ——$O(\varepsilon^{3/2})$

by extending equation (18) to include the $O(\varepsilon^{3/2})$ term (reported in Reference 18). The plots of $\Omega(\xi, \eta)$ corresponding to various orders of $(\varepsilon^{1/2})$ in Figure 3 justify the asymptotic scheme adopted.

Within the range of interest for σ_1 and v

$$0{\cdot}0 < \sigma_1 < 2{\cdot}0$$
$$0{\cdot}0 < v \ < 5{\cdot}0$$

The maximum difference between the $O(\varepsilon^{3/2})$ and the $O(\varepsilon)$ solutions for Ω was always found to be less than 7 per cent. This is reflected in the close agreement between the corresponding curves in Figures 4(a) and 4(b). It can therefore be concluded that truncation of Ω as given by equation (18) yields sufficiently accurate results.

4. THE TIME DEPENDENT EQUATIONS

4.1. The theory

The time dependent stream function Φ can be thought of as an infinitesimal disturbance to the steady state. The equation for $\Phi(\xi, \eta, t)$ can be found by substituting (9) into (6) and assuming that non-linear terms in Φ are sufficiently small to be neglected. We obtain

$$\left\{\frac{1}{R}\left(\mathrm{D}^2 - 4\left(\kappa\frac{\partial}{\partial\xi} + \lambda\frac{\partial}{\partial\eta}\right) + 4(\kappa^2+\lambda^2)\right) - h^2\frac{\partial}{\partial t} - \left(\frac{\partial\Omega}{\partial\eta}\frac{\partial}{\partial\xi} - \frac{\partial\Omega}{\partial\xi}\frac{\partial}{\partial\eta} - 2\kappa\frac{\partial\Omega}{\partial\eta} + 2\lambda\frac{\partial\Omega}{\partial\xi}\right)\right\}\mathrm{D}^2\Phi$$
$$-\left(\frac{\partial\Phi}{\partial\eta}\frac{\partial}{\partial\xi} - \frac{\partial\Phi}{\partial\xi}\frac{\partial}{\partial\eta} - 2\kappa\frac{\partial\Phi}{\partial\eta} + 2\lambda\frac{\partial\Phi}{\partial\xi}\right)\mathrm{D}^2\Omega = 0 \tag{27a}$$

where

$$\Phi = \frac{\partial\Phi}{\partial\eta} = 0, \quad \text{at} \quad \eta = +1 \tag{27b}$$

The coefficients of (27a) are independent of time and are slowly varying with ξ. The stream function of the disturbance, for constant frequency, β, is chosen to be of the form

$$\Phi(\xi, \eta, t) = \phi(\sigma_1, \eta)\exp(\mathrm{i}[\theta(\xi) - \beta t]) + \text{c.c.} \tag{28}$$

where c.c. represents the complex conjugate of the preceding term, and β is chosen to be real.

The slow variation of the coefficients in the ξ-direction is allowed for by the use of a complex wave number $k(\sigma_1)$. This is defined in terms of the complex phase function $\theta(\xi)$ where

$$\frac{\mathrm{d}\theta}{\mathrm{d}\xi} = k(\sigma_1) \tag{29}$$

The expression for the non-dimensional scaling factor h, appearing in equation (27a), may be obtained for the present channel (equation 15) by combining equations (2), (3) and (5), with $\mathrm{d}z/\mathrm{d}\zeta = 1$ at $\zeta = 0$, so that

$$h = \exp\left[\sigma_1 + \varepsilon^{1/2}\frac{m}{2}\sigma_1^2 + \varepsilon^{3/2}\frac{m}{2}\eta^2\right] \tag{30}$$

In the steady state case R and $\varepsilon^{1/2}$ are related through the use of equation (17). However, this relationship is relaxed in this time dependent analysis, with R and $\varepsilon^{1/2}$ assumed to be independent for the purpose of establishing an asymptotic solution to equation (27). Nevertheless, equation (17) is still considered to apply and it is returned to in the final analysis of the results. This artificial relaxation allows the retention of the important viscous term, identified by $1/R$ in equation (27a), in the first order term of the asymptotic expansion for ϕ. This first order term now provides a more accurate approximation to the exact solution than would be the case otherwise. This technique has been used by other authors,[8,20–24] where more detailed explanations are given. In fact a direct numerical approach[9] on the investigations in References 8 and 24 provides another check on the validity of this technique.

The asymptotic development for ϕ takes the form

$$\phi(\sigma_1, \eta; R, m) = \phi_0(\sigma_1, \eta; R, m) + \varepsilon^{1/2}\phi_1(\sigma_1, \eta; R, m) + \varepsilon\phi_2(\sigma_1, \eta; R, m) + \cdots \tag{31}$$

The function ϕ is conveniently normalized by assuming that

$$\phi(0, 0) = 1 \tag{32}$$

and (32) can be equivalently expressed by

$$\phi_0(0, 0) = 1; \quad \phi_i(0, 0) = 0; \quad i \geqslant 1 \tag{33}$$

By substituting (31) into (27a) and comparing powers of $\varepsilon^{1/2}$ once more the following set of equations are obtained.
At $O(1)$ we have

$$\mathrm{L}\phi_0 = 0 \tag{34a}$$

where

$$\phi_0(\sigma_1, \pm 1) = \frac{\partial \phi_0}{\partial \eta}(\sigma_1, \pm 1) = 0 \tag{34b}$$

and

$$\mathrm{L} \equiv \frac{1}{R}(\mathrm{D}_1^2 - k^2)^2 + \mathrm{i}\left(\beta_1 - k\frac{\mathrm{d}G_0}{\mathrm{d}\eta}\right)(\mathrm{D}_1^2 - k^2) + \mathrm{i}k\frac{\mathrm{d}^3 G_0}{\mathrm{d}\eta^3} \tag{34c}$$

with

$$\beta_1 = \beta \mathrm{e}^{2\sigma_1} \quad \text{and} \quad \mathrm{D}_1^2 = \frac{\partial^2}{\partial \eta^2} \tag{34d}$$

This represents the classic Orr–Sommerfeld problem with the frequency, β, and the wave number, k, being replaced by functions of the slow variable σ_1, which are $\beta_1(\sigma_1)$ and $k(\sigma_1)$, respectively. For a given β (real) and fixed σ_1, it is an eigenvalue problem in k.

The higher order equations are of the form

$$\mathrm{L}\phi_i = \Gamma_i; \quad i \geqslant 1 \tag{35a}$$

where

$$\phi_i(\sigma_1, \pm 1) = \frac{\partial \phi_i}{\partial \eta}(\sigma_1, \pm 1) = 0; \quad i \geqslant 1 \tag{35b}$$

The R.H.S. of equation (35a) increases in complexity with each i. In fact

$$\Gamma_1 = \Gamma_1\left(\phi_0, \frac{\partial \phi_0}{\partial \sigma_1}, k_1, \frac{\mathrm{d}k}{\mathrm{d}\sigma_1}\right) \tag{36a}$$

and

$$\Gamma_2 = \Gamma_2\left(\phi_0, \frac{\partial \phi_0}{\partial \sigma_1}, \frac{\partial^2 \phi_0}{\partial \sigma_1^2}, k, \frac{\mathrm{d}k}{\mathrm{d}\sigma_1}, \frac{\mathrm{d}^2 k}{\mathrm{d}\sigma_1^2}, \phi_1, \frac{\partial \phi_1}{\partial \sigma_1}\right) \tag{36b}$$

The exact forms of (36a) and (36b) can be found in References 18 and 19.

The downstream variable σ_1 only appears as a parameter in the homogeneous equation (34a), and so a solution may be found in the form

$$\phi_0(\sigma_1, \eta) = A_0(\sigma_1) f_0(\sigma_1, \eta) \tag{37a}$$

where

$$f_0(\sigma_1, \pm 1) = \frac{\partial f_0}{\partial \eta}(\sigma_1, \pm 1) = 0 \tag{37b}$$

From the theory of homogeneous differential equations,[25] the solution for the non-homogeneous stream functions ϕ_i may be put in the form

$$\phi_i(\sigma_1, \eta) = f_i(\sigma_1, \eta) + A_i(\sigma_1) f_0(\sigma_1, \eta); \quad i \geqslant 1 \tag{38a}$$

where

$$f_i(\sigma_1, \pm 1) = \frac{\partial f_i}{\partial \eta}(\sigma_1, \pm 1) = 0; \quad i \geqslant 1 \tag{38b}$$

Using the normalization given by equation (33) and choosing

$$f_0(\sigma_1, 0) = 1; \quad f_i(\sigma_1, 0) = 0; \quad i \geqslant 1 \tag{39}$$

the complex functions $A_i(\sigma_1)(i \geqslant 0)$ can be interpreted as the amplitudes of ϕ_i along the centre of the channel.

4.2. Numerical solution

The scheme to solve equation (34) is described as follows.

The complex eigenfunction f_0 is an even function in η and hence the boundary conditions (37b) can be replaced by the following conditions for all σ_1.

$$\frac{\partial f_0}{\partial \eta} = \frac{\partial^3 f_0}{\partial \eta^3} = 0, \quad \text{at} \quad \eta = 0 \tag{40a}$$

$$f_0 = \frac{\partial f_0}{\partial \eta} = 0, \quad \text{at} \quad \eta = 1 \tag{40b}$$

Let $u_1(\eta)$ and $u_2(\eta)$ be particular solutions to (34) for fixed σ_1, then

$$f_0(\sigma_1, \eta) = B_1 u_1 + B_2 u_2 \tag{41}$$

where B_1 and B_2 are arbitrary constants for fixed σ_1.

Using (41) and (40b) we obtain

$$B_1 u_1(1) + B_2 u_2(1) = 0 \tag{42a}$$

$$B_1 \frac{\mathrm{d}u_1}{\mathrm{d}\eta}(1) + B_2 \frac{\mathrm{d}u_2}{\mathrm{d}\eta}(1) = 0 \tag{42b}$$

From the theory of homogeneous algebraic equations, a certain characteristic equation must hold for a non-trivial solution to (34). This can be expressed here by insisting that B_1 and B_2 are non-trivial and so

$$u_1(1) \frac{\mathrm{d}u_2}{\mathrm{d}\eta}(1) - u_2(1) \frac{\mathrm{d}u_1}{\mathrm{d}\eta}(1) = 0 \tag{43}$$

This equation defines the eigenrelation for equation (34).

The particular solutions $u_1(\eta)$ and $u_2(\eta)$ are expanded about $\eta = 0$ using a Taylor series satisfying the following conditions at the centre:

$$u_1(0) = 0, \qquad u_2(0) = 1 \tag{44a}$$

$$\frac{\mathrm{d}u_1}{\mathrm{d}\eta}(0) = 0, \quad \frac{\mathrm{d}u_2}{\mathrm{d}\eta}(0) = 0 \tag{44b}$$

$$\frac{d^2u_1}{d\eta^2}(0) = 1, \quad \frac{d^2u_2}{d\eta^2}(0) = 0 \tag{44c}$$

$$\frac{d^3u_1}{d\eta^3}(0) = 0, \quad \frac{d^3u_2}{d\eta^3}(0) = 0 \tag{44d}$$

These conditions are chosen to satisfy equation (40a), otherwise the choice of equations (44a) and (44c) is arbitrary. The fourth derivatives in the expansions for u_1 and u_2 may be obtained using equation (34a). Hence these expansions take the form

$$u_1(\eta) = \frac{\eta^2}{2} + \frac{\eta^4}{24}\left[ikR\frac{dG_0}{d\eta}(0) - iR\beta e^{2\sigma_1} + 2k^2 \right] + \cdots \tag{45a}$$

$$u_2(\eta) = 1 + \frac{\eta^4}{24}\left[ik^2R\beta e^{2\sigma_1} - ikR\frac{d^3G_0}{d\eta^3}(0) - ik^3R\frac{dG_0}{d\eta}(0) - k^4 \right] + \cdots \tag{45b}$$

Assuming that equations (45) describe functions u_1 and u_2 approximately for all η's, substitution in equation (43) yields the following quartic in k, which can be regarding as an approximation to the exact eigenrelation.

$$\frac{k^4}{24} + \frac{iR}{24}\frac{dG_0}{d\eta}(0)k^3 + \left(\frac{1}{3} - \frac{iR}{24}\beta_1\right)k^2 + \frac{iR}{6}\left[\frac{1}{4}\frac{d^3G_0}{d\eta^3}(0) + \frac{dG_0}{d\eta}(0)\right]k + 1 - \frac{iR}{6}\beta_1 = 0 \tag{46}$$

This quartic polynomial with complex coefficients is solved completely for each σ_1 by using a modified Newton–Raphson technique for such polynomials. The complex roots to (46) exhibit an interesting consistency in that one of these always has a positive real part, and the remaining three always have a negative real part. In the context of this problem the physical wave number of the channel is defined by k_r (Real (k)). Thus the approximate root is the one characterized by a positive real part. This consistency may be explained by appealing to the relationships between the roots of the polynomial (46), its coefficients, and the physical constraints of the problem. It is shown in Figure 5 that the real part of the approximate eigenvalue k_0, obtained by using equation (46) becomes closer to the 'exact' value, obtained from the 'exact' solution of the differential equation (34), at large values of σ_1. This property of the approximate solution was used in the numerical iterative scheme employed to obtain a more accurate solution to the eigenvalue problem.

With this initial estimate of k, starting with the maximum value in the σ_1 range, a 'marching' iterative scheme (based on a Runga–Kutta method of order four) was used to solve $u_1(\eta)$ and $u_2(\eta)$. The 'marching' scheme was started at the centre of the channel, $\eta = 0$, where u_1 and u_2 satisfy conditions (44).

With a complete set of u_1's and u_2's computed for this approximate eigenvalue k_0, a function $F(k_0)$ is defined by

$$F(k_0) = u_1(1)\frac{du_2}{d\eta}(1) - u_2(1)\frac{du_1}{d\eta}(1) \tag{47}$$

By defining two more eigenvalues k_1 and k_2 close to k_0, with their respective functions $F(k_1)$, $F(k_2)$, a modified quadratic Newton–Raphson scheme,[26–29] requiring three initial values of k is used to predict a more accurate eigenvalue. The whole process is repeated until this iterative procedure gives a set of u_1's and u_2's which satisfy (43) within the required numerical accuracy. Once the correct eigenvalue has been obtained it then becomes the approximation for the next σ_1, so equation (46) is used only once to obtain an initial guess for k for each different set of R, v and β. The normalization

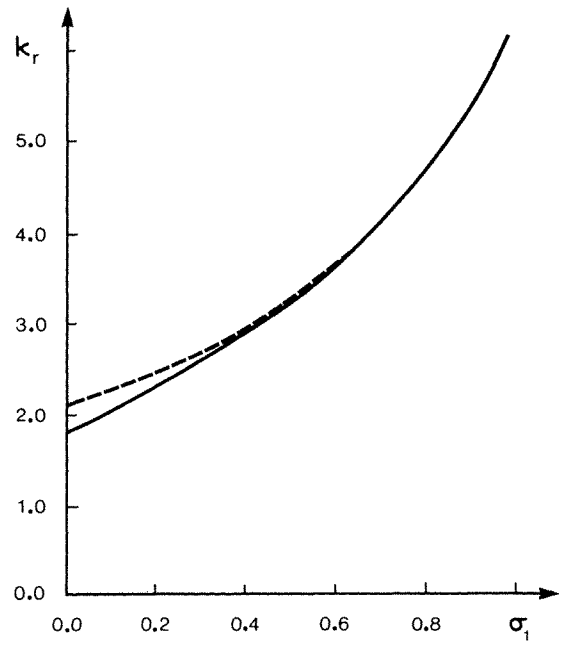

Figure 5. The approximate eigenvalue compared with the correct value for $v = 4{\cdot}093$; $R = 100$, $\beta = 1{\cdot}5$. ——correct, - - - - - approximation

on f_0, (39), and the condition (44a) are sufficient to define B_2, and the boundary conditions (42) at the wall, $\eta = 1$, define B_1. In this way the eigenfunction $f_0(\sigma_1, \eta)$ can be defined completely.

With f_0 obtained it only remains to solve for A_0 in order to define ϕ_0 completely. To solve for A_0 we appeal to a solvability condition on ϕ_1. It can be shown from the theory of non-homogeneous differential equations,[25] that

$$\int_{-1}^{1} \tilde{f}_0 \mathrm{L}\phi_1 \, \mathrm{d}\eta = 0 \tag{48}$$

where $\tilde{f}_0$ is the adjoint eigenfunction of f_0. Using equations (35a) and (36a) for $i = 1$, the solvability condition may be shown[18,19] to reduce to the form

$$\frac{\mathrm{d}A_0}{\mathrm{d}\sigma_1} + H(\sigma_1)A_0 = 0 \tag{49a}$$

and from (33)

$$A_0(0) = 1 \tag{49b}$$

The complex function $H(\sigma_1)$ is defined in terms of definite integrals.[18,19] Integration of equation (49) gives

$$A_0(\sigma_1) = \exp\left[-\int_0^{\sigma_1} H(s)\,\mathrm{d}s \right] \tag{50}$$

In a similar fashion the equations for all subsequent amplitude functions $A_i(\sigma_1)$; $(i \geqslant 1)$ can be found by appealing to the solvability condition on the next order equation for ϕ_{i+1}. The solvability

condition can now be generalized to read

$$\int_{-1}^{1} \tilde{f}_0 \mathrm{L}\phi_{i+1}\,\mathrm{d}\eta = 0; \quad i \geqslant 0 \tag{51}$$

for any function $A_i(\sigma_1)$; $(i \geqslant 0)$. Proceeding as before we obtain for subsequent A_i's

$$\frac{\mathrm{d}A_i}{\mathrm{d}\sigma_1} + H(\sigma_1)A_i = \mathscr{F}_i(\sigma_1); \quad i \geqslant 1 \tag{52a}$$

with

$$A_i(0) = 0 \tag{52b}$$

The complex function $\mathscr{F}(\sigma_1)$ is defined explicitly in References 18 and 19 for the case corresponding to $i = 1$. It can be shown by integrating equation (52a) that

$$A_i(\sigma_1) = A_0(\sigma_1) \int_0^{\sigma_1} \frac{\mathscr{F}_i(s)}{A_0(s)}\,\mathrm{d}s; \quad i \geqslant 1 \tag{53}$$

The particular integrals $f_i(\sigma_1, \eta)$ for the non-homogeneous system (35a) can be expressed[25] for fixed σ_1 by

$$f_i(\sigma_1, \eta) = X_i u_i(\eta) + Y_i u_2(\eta) + U_i(\eta); \quad i \geqslant 1 \tag{54}$$

where u_1 and u_2 are the particular solutions for fixed σ_1 of the previous homogeneous problem, and $U_i(\eta)$ is a particular solution to (35a); X_i, Y_i are constants for some fixed σ_1. The conditions at the wall (38) yield

$$X_i u_1(1) + Y_i u_2(1) + U_i(1) = 0 \tag{55a}$$

$$X_i \frac{\mathrm{d}u_1}{\mathrm{d}\eta}(1) + Y_i \frac{\mathrm{d}u_2}{\mathrm{d}\eta}(1) + \frac{\mathrm{d}U_i}{\mathrm{d}\eta}(1) = 0 \tag{55b}$$

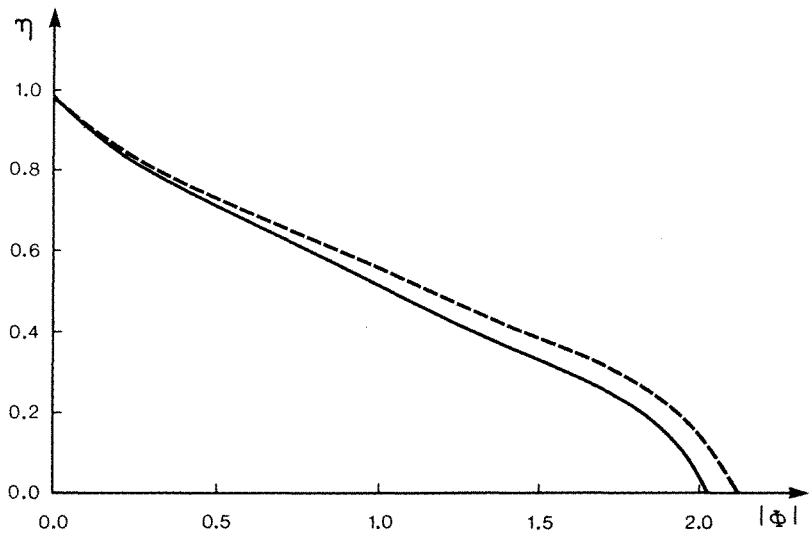

Figure 6. The behaviour of ϕ versus η at $\sigma_1 = 1{\cdot}28$, with and without the $\varepsilon^{1/2}$ correction; $v = 4{\cdot}093$, $R = 30$. - - - - - $|\phi_0|$, —— $|\phi_0 + \varepsilon^{1/2}\phi_1|$

The eigenrelation (43) indicates that equations (55a) and (55b) are not independent, and hence an infinity of solutions exist for X_i and Y_i satisfying (55). Thus in order to find particular solutions of (55), without loss of generality we may choose $Y_i = 0$, and so

$$X_i = -\frac{U_i(1)}{u_1(1)} = -\frac{\mathrm{d}U_i(1)/\mathrm{d}\eta}{\mathrm{d}u_1(1)/\mathrm{d}\eta} \tag{56}$$

The function $U_i(\eta)$ can be computed using a Runga–Kutta method similar to that described for $u_1(\eta)$ and $u_2(\eta)$.

It can be seen that the complexities of the formulations and their solutions increase dramatically with increasing order of terms in equation (31). For this reason and for the requirements of the present solution, it was found sufficient to truncate equation (31) up to and including the ϕ_1 term. However, the function f_2 was computed for the purpose of checking the accuracy of the amplitude function $A_1(\sigma_1)$. In general, the value of $f_i (i \geqslant 1)$ is accurate when the condition given in (56) is satisfied, which in turn also serves as a check on the amplitude function $A_{i-1}(\sigma_1)$. To define ϕ_2 completely would mean solving the equation for $A_2(\sigma_1)$, and this can only be obtained by using the solvability condition on ϕ_3 (51).

In Figure 6 the effect of including ϕ_1 in the asymptotic expansion (31) is illustrated. The maximum observed difference between $|\phi_0|$ and $|\phi_0 + \varepsilon^{1/2}\phi_1|$ at a position downstream defined by $\sigma_1 = 1{\cdot}28$, is approximately 13 per cent.

5. DISCUSSION

The preceding sections have provided the theoretical basis, and the numerical techniques necessary to solve the Navier–Stokes equations for the steady state, $\Omega(\xi, \eta)$, and time dependent, $\Phi(\xi, \eta, t)$, stream functions, for flow in a symmetric curved walled channel. In fact this solution for the curved walled channel given by (15) provides the solution for straight walled channels on setting $m = 0$ or in the asymptotic sense $\varepsilon^{1/2} \to 0$, σ_1, η, m fixed. The solution also contains the Poiseuille case when $\varepsilon^{1/2} = 0$.

The perturbation scheme employed to solve the non-linear differential equation for $G_0(\eta)$ gave accurate results even for relatively high values of the perturbation parameter v. In fact a value of $v = 5$ was used in a parametric study to optimize the number of perturbation terms and η steps required.

The occurrence of the Orr–Sommerfeld problem in stability studies makes an independent and automatic iterative scheme more desirable than purely searching routines, or routines that rely on drawing information from other investigations.

The full potential of the results with higher order terms and curvature included, may be realized in a stability study.[18,19] In fact these results would facilitate a stability study of the spatial growth of the disturbance up to and including the $O(\varepsilon)$ term. We note that ϕ_2 is not necessary for such a study[18,19] and its solution would only be necessary if the stability study were to include the $O(\varepsilon^{3/2})$ terms, which in this case would be prohibitively complicated.

The stability analysis would involve finding the critical Reynolds number at each local point, and using the minimum of these to determine the overall R_{crit}. By local R_{crit} we mean that the local growth of the disturbance in the streamwise direction can occur for some values of the frequency β when $R > R_{\text{crit}}$, local, but now growth can occur for any β when $R < R_{\text{crit}}$, local. In any analysis of the results the relationship (17) which was relaxed in the time dependent analysis would be returned to.

The theory can be applied to a number of symmetric curved walled channels. In Figure 7 an accurate representation of the channel generated by defining $\alpha(\tau) = \varepsilon^{1/2} m_1 \operatorname{sech}^2 \tau$, is given. This

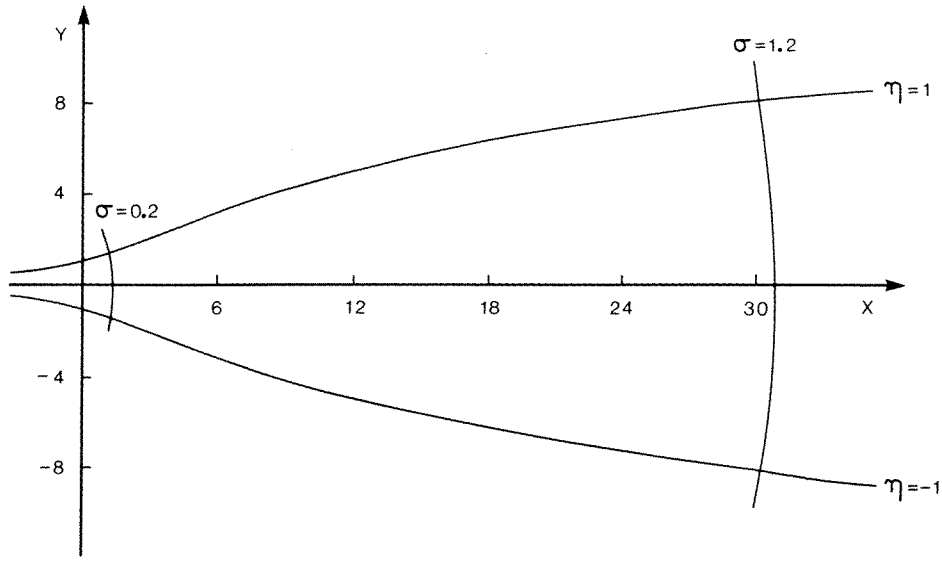

Figure 7. A curved walled channel given by $\alpha(\tau) = \varepsilon^{1/2} m_1 \operatorname{sech}^2 \tau$ with $m_1 = 1$ and $\varepsilon^{1/2} = 0{\cdot}4$

channel is within experimental dimensional limits, and its bottle-neck feature would exhibit nearly Poiseuille flow far upstream and downstream with Jeffery–Hamel type flow near a region where the angle of divergence reaches a maximum. An additional channel with physically interesting features is given in Figure 8, this is a schematic representation of $\alpha(\tau) = \varepsilon^{1/2} m_2 \tau/(1+\tau^2)$. This channel may be of interest as it contracts then dilates in a manner similar to a Venturi tube.

A stability study of it would follow the lines of the channel presented in Figure 7, the results of which may be found in References 18 and 19.

A few velocity profiles have also been included in Figure 8 to demonstrate that we expect the flow to be initially like Poiseuille (A), then, as the channel contracts, the velocity at the centre decreases

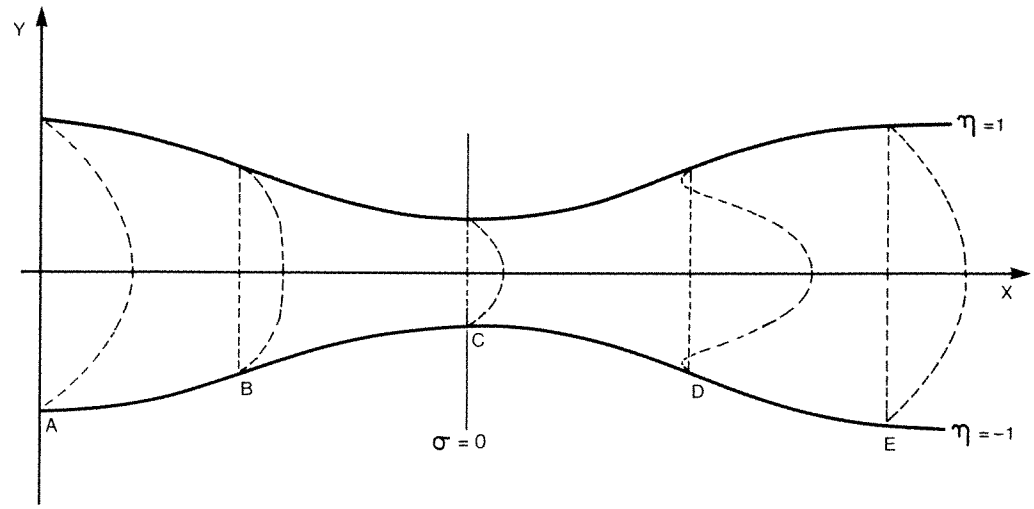

Figure 8. A curved walled channel characterized by $\alpha(\tau) = \varepsilon^{1/2} m_2 \tau/(1+\tau^2)$. (The velocity profiles are not to scale)

(B), and near the region $\sigma = 0$ it resumes nearly Poiseuille flow again (C). As the channel dilates, the flow becomes increasingly more like Jeffery–Hamel flow where separation may take place, and finally ending with nearly Poiseuille flow again (E).

Fraenkel[1,2] states that these slowly varying channels are characterized by the property

$$C(\xi) = |(\text{local wall curvature}) \times (\text{local channel width})| \leqslant \varepsilon_0 \tag{57}$$

where $C(\xi)$ is a dimensionless wall curvature function, and the asymptotic expansion is expressed as some power of ε_0. Fraenkel goes on to show that if the parameters in the definition of $\alpha(\tau)$, equation (15), are such that

$$\frac{d\alpha(\sigma)}{d\sigma} \leqslant 1 \tag{58}$$

then

$$\varepsilon_0 = 2\varepsilon \tag{59}$$

Under these circumstances the local wall curvature at $\eta = 1$, (λ/H), may be shown to satisfy

$$\frac{\lambda}{H} \leqslant \frac{\varepsilon}{H}$$

and since $H = bh$ has a minimum value when $\sigma_1 = 0$, (30), then the maximum curvature which can be admitted is given by $(h = 1)$

$$\frac{\lambda}{H} \leqslant \frac{\varepsilon}{b} \tag{60}$$

6. CONCLUDING REMARKS

We have provided asymptotic and numerical schemes for the solution of the steady state and time dependent stream functions, for flows in symmetric channels with small wall curvature. In these schemes a class of non-linear functions appear as first order approximations to the basic flows, and the Orr–Sommerfeld equation appears as the first order problem for small disturbances to these basic flows.

The numerical and perturbation methods have produced consistent results, and where comparisons could be made, these results agree well with other published results.

To test the validity of this stability theory experimentally, it would be necessary to choose an appropriate $\alpha(\tau)$ which not only satisfied the constraints of the theory, but was also practical enough to be constructed in the laboratory. The channels presented in Figures 7 and 8 offer two such choices.

It can therefore be seen that the theoretical and numerical analyses presented here have applications in stability studies for the class of channels considered, and other symmetric channels satisfying the required constraints.

LIST OF SYMBOLS

a_1, a_2	general orthogonal co-ordinates
$A_i(\sigma_1)$	amplitude functions for the disturbance stream functions $\phi_i(\sigma_1, \eta)$.
b	a length scale, approximately half the throat width

$f_0, \bar{f}_0$	the eigenfunction (f_0) and the adjoint eigenfunction
f_1, f_2	solutions to the $O(\varepsilon^{1/2})$, and $O(\varepsilon)$ disturbance equations, respectively
$G_i(\eta)$	terms in the steady state stream functions $\Omega_i(\xi, \eta)$
$h(\xi, \eta)$	non-dimensional scaling factor
h_1, h_2	general orthogonal dimensionalized scaling factors
$H(\xi, \eta)$	dimensional scaling factor
$H(\sigma_1)$	coefficient in the amplitude equation for $A_0(\sigma_1)$
$k(\sigma_1)$	complex wave number.
L	operator in the $O(1)$ disturbance equation
m, m_1, m_2	curvature parameters.
M	half the volumetric flow rate
R	the Reynolds number M/ν
t	non-dimensional time
T	dimensional time
$u_1(\eta), u_2(\eta)$	solutions to the $O(1)$ disturbance equations
v	parameter defining the Jeffery–Hamel profiles
$w_i(\eta)$	perturbation functions
x	non-dimensional x-Cartesian co-ordinate
X	dimensional x-Cartesian co-ordinate
y	non-dimensional y-Cartesian coordinate
Y	dimensional y-Cartesian coordinate
z	$x + \mathrm{i}y$
Z	$X + \mathrm{i}Y$
$\alpha(\sigma_1)$	like the semi-divergence angle of the channel walls
β	a real frequency
β_1	the intrinsic real frequency
ε	The parameter characterizing the slow variation
ζ	the non-dimensional complex variable ($= \xi + \mathrm{i}\eta$)
η	the non-dimensional transverse co-ordinate
$\theta(\xi)$	the complex phase function
$\vartheta(\xi, \eta)$	the angle between corresponding line elements in the Z, ζ plane
κ, λ	like the curvatures of the lines in the plane
$\mu(\zeta)$	the complex function generating symmetric channels
ν	the kinematic viscosity
ξ	the non-dimensional downstream co-ordinate
σ	the slow-downstream variable ($= \varepsilon\xi$)
σ_1	the slow downstream variable ($= \varepsilon^{1/2}\xi$)
τ	the slow complex variable ($= \varepsilon\zeta$)
$\phi(\sigma_1, \eta)$	the time-independent disturbance stream function
$\phi_0(\sigma_1, \eta), \phi_1(\sigma_1, \eta), \phi_2(\sigma_1, \eta)$	the time-independent disturbance stream functions of $O(1)$, $O(\varepsilon^{1/2})$, and $O(\varepsilon)$, respectively
$\phi(\xi, \eta, t)$	the time-dependent disturbance stream function
$\psi(\xi, \eta, t)$	the non-dimensional total stream function $= \Omega + \Phi$
$\hat{\Psi}(\xi, \eta, t)$	the dimensional total stream function
$\Omega(\xi, \eta)$	the steady state stream function
$\Omega_0, \Omega_1, \Omega_2, \Omega_3$	the $O(1)$, $O(\varepsilon^{1/2})$, $O(\varepsilon)$ and $O(\varepsilon^{3/2})$ steady state stream functions, respectively

APPENDIX I

The asymptotic expansion for $\Omega(\xi, \eta)$ takes the form

$$\Omega(\xi, \eta; v_1 m) = \Omega_0(\sigma, \eta; v_1 m) + \varepsilon^{1/2}\Omega_1(\sigma, \eta; v_1 m) + \varepsilon\Omega_2(\sigma, \eta; v_1 m) + \cdots \tag{61}$$

In turn Ω_0, Ω_1 and Ω_2 are expanded in a Taylor series about $\sigma = 0$ using $\sigma = \varepsilon^{1/2}\sigma_1$. New functions are introduced such that

$$\Omega_0 = \chi_0(\sigma_1, \eta; v, m) = G_0(\eta; v) + \varepsilon^{1/2}\sigma_1 G_1(\eta; v, m) + \varepsilon\sigma_1^2 G_2(\eta; v, m) + \cdots \tag{62}$$

$$\Omega_1 = \chi_1(\sigma_1, \eta; v, m) = G_3(\eta; v) + \varepsilon^{1/2}\sigma_1 G_4(\eta; v, m) + \cdots \tag{63}$$

$$\Omega_2 = \chi_2(\sigma_1, \eta; v, m) = G_5(\eta; v) + \cdots \tag{64}$$

There is no need to go any further in (63) and (64) since χ_1 and χ_2 are multiplied by $\varepsilon^{1/2}$ and ε respectively in (61). The final form for Ω is found by substituting (62), (63) and (64) into (61) and ordering the terms.

APPENDIX II

The central difference expressions for the derivatives up to the fourth derivative of $O(h^4)$ used for the discretization of equations (23a) and (24a) are

$$\frac{dy_i}{d\eta} = \frac{1}{12h}(-y_{i-2} - 8y_{i-1} + 8y_{i+1} - y_{i+2}) \tag{65}$$

$$\frac{d^2y_i}{d\eta^2} = \frac{1}{12h^2}(-y_{i-2} + 16y_{i-1} - 30y_i + 16y_{i+1} - y_{i+2}) \tag{66}$$

$$\frac{d^3y_i}{d\eta^3} = \frac{1}{8h^3}(y_{i-3} + 8y_{i-2} + 13y_{i-1} - 13y_{i+1} + 8y_{i+2} - y_{i+3}) \tag{67}$$

$$\frac{d^4y_i}{d\eta^4} = \frac{1}{6h^4}(-y_{i-3} + 12y_{i-2} - 39y_{i-1} + 56y_i - 39y_{i+1} + 12y_{i+2} - y_{i+3}) \tag{68}$$

APPENDIX III

A consistent method for discretizing boundary conditions is to derive the finite difference expressions from the same polynomial. In this case an 8th order polynomial was used at $i = N$ (see Figure 2), so that

$$w_r(\eta) = w_r(N) + \frac{dw_r}{d\eta}(N)\eta + \frac{1}{2!}\frac{d^2w_r}{d\eta^2}(N)\eta^2 + \cdots + \frac{1}{8!}\frac{d^8w_r}{d\eta^8}(N)\eta^8 + \cdots \tag{69}$$

The necessary derived finite difference expressions are

$$\frac{dw_r}{d\eta}(N) = \frac{1}{60h}[-w_r(N-3) + 9w_r(N-2) - 45w_r(N-1) + 45w_r(N+1) - 9w_r(N+2) + w_r(N+3)] + A_1h^6\frac{d^7w_r}{d\eta^7}(N) \tag{70}$$

$$\frac{d^2w_r}{d\eta^2}(N) = \frac{1}{90h^2}[w_r(N-3) - 13{\cdot}5w_r(N-2) + 135w_r(N-1) - 245w_r(N) + 135w_r(N+1) - 13{\cdot}5w_r(N+2) + w_r(N+3)] + A_2h^6\frac{d^8w_r}{d\eta^8}(N) \tag{71}$$

$$\frac{d^4 w_r}{d\eta^4}(N) = \frac{1}{6h^4}[-w_r(N-3) + 12w_r(N-2) - 39w_r(N-1) + 56w_r(N) - 39w_r(N+1) + 12w_r(N+2) - w_r(N+3)] + A_4 h^4 \frac{d^8 w_r}{d\eta^8}(N) \tag{72}$$

$$\frac{d^5 w_r}{d\eta^5}(N) = \frac{1}{2h^5}[-w_r(N-3) + 4w_r(N-2) - 5w_r(N-1) + 5w_r(N+1) - 4w_r(N+2) + w_r(N+3)] + A_5 h^2 \frac{d^7 w_r}{d\eta^7}(N) \tag{73}$$

Here h is the grid spacing, and A_1, A_2, A_4 and A_5 are discretization error constants. The consistency of this method lies in the fact that all derivatives have been derived from the same order polynomial, in this case an $O(8)$ polynomial.

REFERENCES

1. L. E. Fraenkel, 'Laminar flow in symmetric channels with slightly curved walls, I. On the Jeffery–Hamel solutions for flow between plane walls', *Proc. Roy. Soc. A*, **267,** 119 (1962).
2. L. E. Fraenkel, 'Laminar flow in symmetric channels with slightly curved walls II. An asymptotic series for the stream function', *Proc. Roy. Soc. A*, **272,** 406 (1963).
3. G. B. Jeffery, 'The two dimensional steady motion of a viscous fluid', *Phil. Mag.*, **29,** (6), 455 (1915).
4. G. Hamel, 'Spiralförmige Bewegungen zäher Flüssigkeiten', *Jber. dtsch. Matver.*, **25,** 279 (1917).
5. L. Rosenhead (Ed.), *Laminar Boundary Layers*, Oxford, 1963.
6. D. J. Benney and S. Rosenblat, 'Stability of spatially and time-dependent flows', *Phys. of Fluids*, **7,** 1385 (1964).
7. R. D. Lucas, *Ph.d Thesis*, Stanford University, 1972.
8. P. M. Eagles and M. A. Weissman, 'On the stability of slowly varying flow: the divergent channel', *J. Fluid Mech.*, **69,** 241 (1975).
9. M. Allmen, *Ph.d Thesis*, The City University, The Department of Mathematics, 1980.
10. J. Watson, 'On spatially-growing finite disturbances in plane Poiseuille flow', *J. Fluid Mech.*, **14,** 211 (1962).
11. P. M. Eagles, 'The stability of a family of Jeffery–Hamel solutions for divergent channel flow', *J. Fluid Mech.*, **24,** 191 (1966).
12. W. Heisenberg, 'Über Stabilität and Turbulenz von Flüssigkeitsströmen', *Ann. Phys., Lpz.*, **74,** (4), 577 (1924). Translated as 'On the stability and turbulence of fluid flows', *Tech. Memor. nat. adv. Comm. Aero.*, Wash. No. 1291.
13. O. G. Tietjens, 'Beiträge zur Entstehung der Turbulenz', *Z. angew. Math. Mech.*, **5,** 200 (1925).
14. W. Tollmien, 'Über die Enstehung der Turbulenz', *Nachr. Ges. Wiss.*, Göttingen, 21 (1929).
15. H. Schlichting, 'Zur Enstehung der Turbulenz bei der Plattenströmung', *Nachr. Ges. Wiss.*, Göttingen, Math. Phys. Klasse, no. 181–208 (1933).
16. L. H. Thomas, 'The stability of plane Poiseuille flow', *Phys. Rev.*, **91,** (2), 780 (1953).
17. S. Goldstein (Ed.), *Modern Developments in Fluid Dynamics*, Clarendon Press, Oxford, 1938.
18. G. A. Georgiou, *Ph.d Thesis*, The City University, Department of Mathematics, 1982.
19. G. A. Georgiou and P. M. Eagles, 'The stability of flows in channels with small walled curvature', to be published (1985).
20. M. Gaster, 'On the effects of the boundary layer growth on flow stability', *J. Fluid Mech.*, **66,** 465 (1974).
21. M. Bouthier, 'Stabilité linear des écoulments presque parallèles', *J. Méchanique*, **11,** 599 (1972) and **12,** 75 (1973).
22. C. H. Ling and W. C. Reynolds, 'Non-parallel flow corrections for the stability of shear flows', *J. Fluid Mech.*, **59,** 571 (1973).
23. H. Lanchon and W. Eckhaus, 'Sur l'analyse de la stabilité des écoulments faiblement divergents', *J. de Méchanique*, **3,** 445 (1964).
24. P. M. Eagles and F. T. Smith, 'On the steady flow and its stability in certain channels with slowly varying width', *J. Eng. Math.*, **14,** (3), 219 (1980).
25. E. L. Ince, *Ordinary Differential Equations*, Dover Publications, 1956.
26. A. Ralston, *A First Course in Numerical Analysis*, McGraw-Hill, 1965.
27. D. E. Muller, 'A method of solving algebraic equations using an automatic computer', *MTAC*, **10,** 208 (1956).
28. A. M. Ostrowski, *Solutions of Equations and Systems of Equations*, Academic Press Inc., New York, 1960.
29. J. F. Traub, *Iterative Methods for the Solution of Equations*, Prentice-Hall Inc. 1964.